

# EFFECT OF GAS NITRIDING PARAMETERS ON THE MICRO-HARDNESS OF HIGH-SPEED STEEL-CUTTING TOOLS

Falah Mustafa Al-Saraireh\*, Shatha Adel Suhymat

Mutah University, Faculty of Engineering, Mechanical Engineering Department, Karak, Jordan

\*f\_saraireh@mutah.edu.jo

*In this study, the nitriding parameters, such as nitriding time, nitrogen flow, and cooling type, were regularly modified to assess the effects of each on the microhardness of tools constructed of high-speed steel designed for commercial usage. The nitriding temperature was maintained at 670 °C for all of the tools. The tools were designed to measure microhardness. With a maximum value of 2000 HV at a time of 42 hours, direct nitriding with a nitrogen flow of 20 l/h and air cooling exhibits an apparent relationship between nitriding time and microhardness. The maximum microhardness value (1555.44 HV) was achieved by quenching after nitriding for 72 hours with a nitrogen flow rate of 20 l/h. The relationship between nitrogen flow and microhardness is semi-direct for direct nitriding at a nitriding duration of 30 hours and furnace cooling, with a maximum value of 1566.65 HV at a nitrogen flow of 110 l/h. The maximum microhardness was 2000 HV, with a 1.63% increase. The microstructure of the tools was improved by increasing the concentration of iron nitride in the ferrite cell, which means that the gas nitriding process increases the efficiency of cutting operations and reduces workpiece material surface roughness, based on the results of this study, it is advised to use high-purity nitrogen rather than ammonia. high-purity nitrogen gives better results than traditional nitriding using ammonia gas.*

*Keywords: nitriding, microhardness, machining operations, cutting tool, heat treatment*

## 1 INTRODUCTION

When the manufacturer utilizes the cutting tool, it is supposed to be hard and resist wear to increase the tool life [1], and reduce the waste of machined material, so it is necessary to search for harnessing reinforcement to enhance the mechanical properties and the efficiency of the cutting tool on another hand the need for quality [2], at the same time, the economy and saving money.

Nitriding is one of the most important heat treatment procedures due to the diffusion of nitrogen (N), which is used to harden the surface of the ferrous metal or alloy and improve the mechanical properties while increasing the cutting tool life [3]. Nitriding is a widely used heat treatment operation to the surface of the metal to improve its mechanical properties as the resistance to wear, fatigue, and corrosion [4].

The control of nitriding process parameters gives the super results to enhance the material characteristics. In nitriding, the nitrogen (N) leaves its chemical compound i.e. (Ammonia  $\text{NH}_3$ ) atmosphere and reacts with the material, metal, or alloy surface to give a compound layer (White layer) above the diffusion zone over the surface of the material [5], these two layers are new solid-state structure with properties that impossibly to get in each one separately e.g., nitriding steel compound layer is  $\epsilon - \text{Fe}_{2-3}$ , and  $\gamma - \text{Fe}_4\text{N}$  phases [6]. The temperature of the nitriding process must be below the maximum tempering temperature of the cutting tool material to prevent the softening of the tool i.e. (tool steel nitriding temp.  $\sim 600$  °C). [7]

The compound layer improves wear and corrosion resistance, the diffusion layer improves fatigue endurance, and the final product surface finish will be better [8]. In the diffusion zone, the nitrogen occupies interstices in the tool surface,

For effective cutting operations, the material of the cutting tool must be harder than the material of the work part [9]. Turning cutting operations use a cutting tool with a single point to generate a cylindrical shape of the workpiece.

### 1.1 Types of cutting tool wear

The top rake face and the flank of the cutting tool both experience four types of wear, which can be categorized into:

- The crater wears a concave part of the rake face resulting from the chip sliding against the surface [10].
- Between the new workpiece surface and the flank relief face close to the cutting edge, flank wear (flank wear band) occurs.
- Notch wear: The cutting tool edge located closest to the original surface of the workpiece experiences the greatest amount of wear. This is because the original surface of the workpiece is harder than the internal surface of the work material as a result of hardening, prior machining, or possibly sand particles from casting, among other factors [11].
- Nose radius wear: This resulted in a cutting edge in the nose radius.

## 1.2 The mechanism of cutting tool wear

- Abrasion: Tough particles in the workpiece wear down the cutting tool, causing crater wear or flank wear, for instance [12].
- Adhesion: contact between two metals at a high temperature and pressure (similar to welding); in cutting operations, adhesion is embodied when the chip travels along the cutting tool's rake face and takes a small amount of the tool with it [13].
- Diffusion: Diffusion happens when the chip and the tool come into contact. As a result, the tool's surface loses some of its atoms, which gives it its hardness. Over time, the tool will gradually come into touch with wear [14].
- Plastic deformation: causes the tool material to become weaker when it deforms plastically at high temperatures, which contributes to wear [15].

The main advantage of utilizing nitriding for cutting tools is that it results in the least amount of tool wear due to the above-mentioned wear mechanisms, which increase with high temperature and high cutting speed [16].

## 1.3 Nitriding parameters

Temperature, time, and nitriding environment are the three nitriding parameters that influence this process [17]. To avoid softening the tool, the temperature during the nitriding operation must be lower than the highest temper temperature of the cutter's materials [18]. For example, the tool steel should be nitriding at a temperature of about 600 °C [19]. The diffusion layer increases fatigue endurance, the compound layer enhances wear and corrosion resistance, and the final product will have a superior surface polish. Nitrogen fills in the gaps in the tool surface within the diffusion zone [20]. The processes involved in nitriding can be classified into the following categories related to the nature of the nitrogen environment:

- Gas nitriding: The most effective method to improve the tool surface, especially for complex shapes that need identical hardening of the tool surface [21].
- Plasma nitriding (ion nitriding): This process uses plasma discharge technology, it is also another hardening process at low temperatures, the word plasma means that ionized gas consists of positive ions and free electrons, plasma is generated in a vacuum by high-voltage electrical energy, this plasma runs into the negative pole-cutting tool [22]. The ion collision cleans the surface facilitates the nascent nitrogen to be distributed in the cutting tool material, and also increases the temperature of the tool [23].
- Packed nitriding: This process uses organic substances, the cutting tool, and nitrogen Compound packed in glass-ceramic or aluminum containers, the internal environment of the container is filled with Organic nitrogen and then heated approximately to 750 °C, the reaction starts, and nitrogen is produced to complete the nitriding process, it takes from two hours to sixteen hours [24].
- Salt bath nitriding: Utilized for carbon steel, low alloy steel, stainless steel, cast iron, and nitrogen-containing molten salt medium, the tool's dimensional stability can be preserved, allowing it to process the final nitriding [25].

For this investigation, nitriding (the most significant surface heat treatment) was selected. to investigate the effects of temperature, time, and nitriding environment on the cutting tool's hardness and life [26]. Studying the effect of nitriding with its various variables on the cutting tool is of great importance in improving the cutting process [27], saving a lot of time and effort, and increasing the quality of the pieces produced at the lowest possible costs [28]. One of the main causes of cutting tool material consumption is wear of all kinds. As a heat treatment method, nitriding should be applied to reduce wear and improve the characteristics of cutting tools [29].

Researchers have studied cutting tool material over the years to improve cutting efficiency and produce accurate products with high precision. In this study the nitriding process 'the most important surface heat treatment' was chosen, and how these process parameters (temperature, time, nitriding atmosphere) affect the tool life and the hardness of the cutting tool in addition to the characteristics of the final product surface finish and the grain shape of both contacting materials. Because machinability parameters are unrelated to one another, obtaining specific measurements of material machinability is difficult, as a result, craftsmen rely on machining recommendations derived from experimental testing and data collected by manufacturing industries. Studying the effect of nitriding with its various variables on the cutting tool is of great importance in improving the cutting process, saving a lot of time and effort, and increasing the efficiency of the pieces produced at the lowest possible costs. One of the main causes of cutting tool material consumption is wear of all kinds. Nitriding should be used as a heat treatment procedure to decrease wear and enhance cutting tool properties.

## 2 MATERIALS AND METHODS

One piece of a high-speed steel cutting tool (10×10×100) mm, was used in this study, and analyzed by (SEM-EDX, company: FEL, Model: Quanta 600) device [28] in Environment Water and Energy Research Center (EWERC) /Al al-Bayt University /Al-Mafraq, Jordan, and the results are shown in Table 1.

Table 1. Tool Chemical Analysis Weight%

Sample specification					
Material symbol	C	Si	Fe		
Percentage content%	3.14	0.32	96.54		
Sample line					
Material symbol	C	O	K	Cr	Fe
Percentage content %	2.53	0.56	0.14	3.64	93.13
Sample spot					
Material symbol	C	Si	Cr	Mn	Fe
Percentage content %	1.17	0.31	6.00	0.70	91.82

### 2.1 Cutting tools wear data

To accelerate tool wear, the wear test is performed before and after the nitriding process using a high rotational speed lathe machine at fixed conditions (rotational speed 1000 rpm, length of cut 5 cm, depth of cut 1 cm, for 5 seconds with water cooling).

Because the turning operation is done with cooling the heat generation effect due to friction is very little and can be neglected.

The goal of this process is to make a difference in the weight of the tool so that we can monitor it and calculate the wear loss per time that occurred, which gives an impression of the tool's life, so the lower the wear loss, the longer tool life, and vice versa. The weight was measured before and after the turning operation for two cutting tools, one before nitriding and the other chosen randomly after nitriding (tool no. K11), as shown in Table 2.

Table 2. The tool's weight differences

Tool	Weight before turning $W_1$ (g)	Weight after turning $W_2$ (g)	Weight loss= $W_1-W_2$ (g) (Rotational speed 1000 rpm, length of cut 5 cm, time 5 seconds with water cooling)
Before nitriding	59.5813	59.5809	0.0004
After nitriding	60.7307	60.7305	0.0002

### 2.2 Nitriding parameters settings

To organize the inspection process for the cutting tools according to the gas nitriding conditions, a symbol was given to each piece as illustrated in Table 3. In this study, three nitriding parameters were considered:

Nitriding time, nitrogen flow, and cooling type [30]. Experiments were set up by changing these three parameters to study the effect of each on the cutting tool's hardness. After taking the specimens out of the furnace, tests were performed on all of them, and the results were illustrated in tables to facilitate studying and comparing the results. To accelerate tool wear, the wear test was performed before and after the nitriding process using a high rotational speed lathe machine at fixed conditions (rotational speed 1000 rpm, length of cut 5 cm, depth of cut 1 cm, for 5 seconds with water cooling) [30].

Table 3. Cutting tools nitriding parameters

Specimen Symbol	Nitriding Time (h)	Cooling type	Nitrogen flow (l/h)	Heat treatment before nitriding
A1	None	None	None	None
N11	6	Air cooling	20	None
O11	12	Air cooling	20	None
P11	18	Air cooling	20	None
C11	24	Air cooling	20	None
K11	30	Air cooling	20	None
E11	42	Air cooling	20	None
M11	48	Air cooling	20	None
G11	56	Air cooling	20	None

Specimen Symbol	Nitriding Time (h)	Cooling type	Nitrogen flow (l/h)	Heat treatment before nitriding
D11	72	Air cooling	20	None
F11	72	Furnace cooling	20	None
J11	72	Oil quenching	20	None
I11	18	Air cooling	50	Tempered
Sh-5	24	Air cooling	50	Tempered
Sh-4	30	Air cooling	50	Tempered
Sh-3	24	Furnace cooling	20	Tempered
Sh-2	24	Air cooling	50	None
Sh-1	18	Air cooling	110	Tempered
A11	24	Furnace cooling	80	None
H11	24	Furnace cooling	110	Tempered
Q11	30	Furnace cooling	20	Tempered
L11	18	Furnace cooling	20	Tempered
B11	30	Air cooling	110	Tempered

### 3 RESULT AND DISCUSSION

Based on the parameters of the nitriding process, the treated cutting tools were grouped into eight groups from 1 to 8. And since the nitriding process means the spread of nitrogen, and its penetration into the steel material to produce nitrogen carbides, then the greatest effect of nitration will be visible on the outer surface of the sample, so this must be taken into account when inspecting the microstructure of the cutting tool and focusing on the area of the edges close to the surface of the sample, especially at the corners.

#### 3.1 Specimens' groups

##### 3.1.1 Group no. 1

The measured values of hardness for group no.1 shown in Fig. 1 appear to rise beginning with (757.76 HV) before treatment and after curing for six hours to (759.08 HV). As a result of the previously mentioned findings, it is noticed that the nitriding period must be set to an appropriate limit to achieve the highest possible hardness values.

As the nitriding time increased, hardness increased steadily till it reached its maximum value of 2000 HV at 42 h. After that, it started to decline once more, reaching its lowest value of 795.93 HV at 72 h. This value is very close to the initial value before the gas nitriding operation began. In terms of micro-hardness, the best value is recorded at 42 h (2000 HV), while the lowest value is recorded at 6 h (757.08 HV). Hardness levels in this set of tools began to drop at a nitriding time of 42 h, an unexpected outcome of the procedure that theoretically increases hardness with time.

The result can be explained as follows: when the tool surface reaches a certain point (42 h into the nitriding process), the reactions between the ferrite and nitrogen gas stop, and extending the nitriding time above 42 h is not as beneficial. Conversely, it yields the opposite outcome. As a result, expanding the nitriding time needs to be carefully considered to provide the greatest hardness results. This is the intended outcome to increase the cutting tool's lifetime and efficiency.

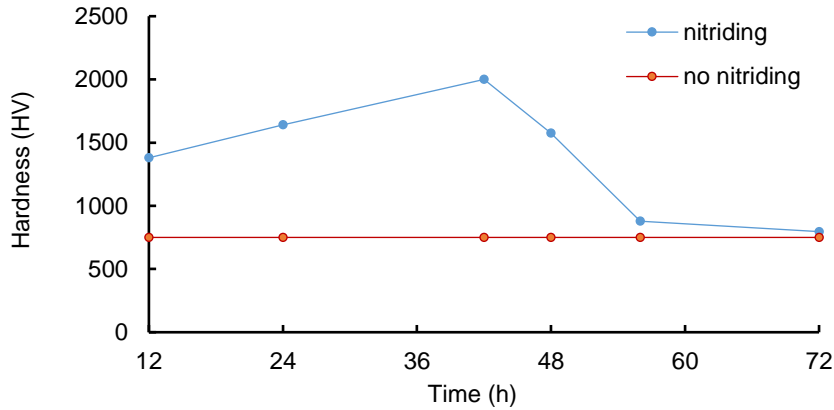


Fig. 1. The effect of nitriding time on hardness for group 1 (670 °C, 20 l/h, air cooling)

As shown in Fig. 2 the inner structure of the tool has become more organized and arranged, and the microstructure has changed from a ferrite to a martensitic microstructure. This was taken with a precision of 70 μm. observed when snapshots were taken.

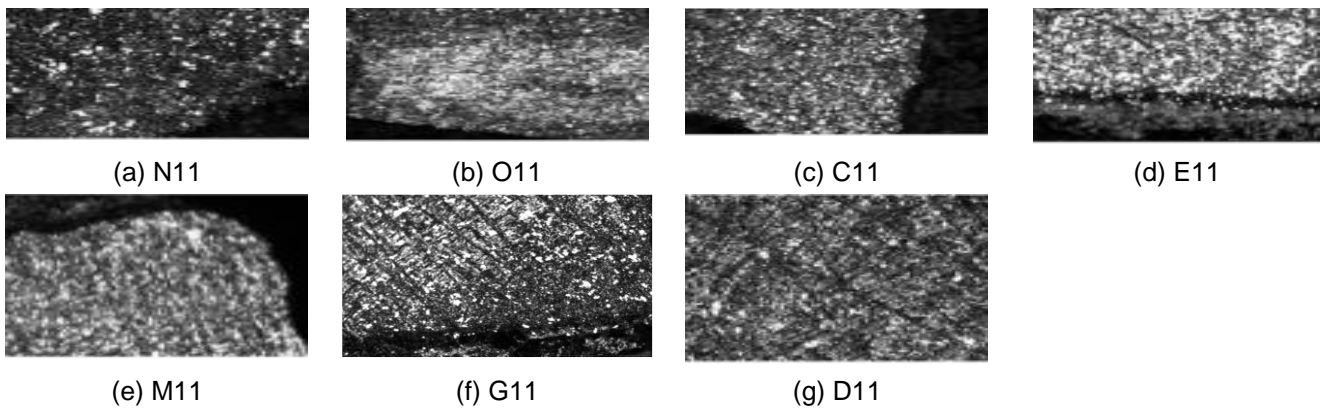


Fig. 2. The microstructure of group 1 (670 °C, 20 l/h, air cooling)

### 3.1.2 Group no. 2

As seen in Fig. 3 down below, the micro-hardness of the tool at 18 h is the highest (839.36 HV), while at 30 h it is the lowest (717.95 HV). At 30 h, the micro-hardness reduced slightly in comparison to the untreated tool. The micro-hardness at (tempered, 670 °C, 50 l/h, air cooling) decreases with time. This can be explained by the fact that, at 50 l/h, the tool surface is nitrided more quickly, allowing the white layer to become weaker over time and leading to a decrease in hardness.

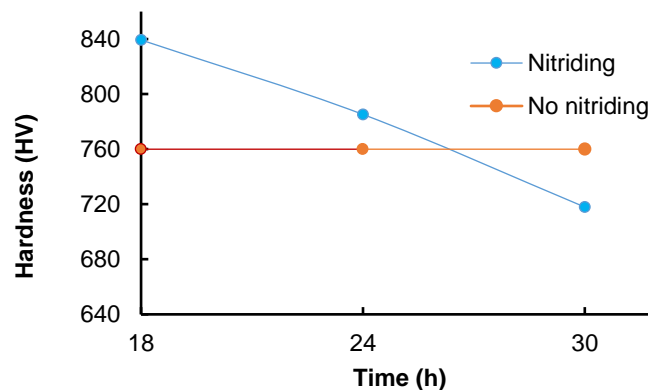


Fig. 3. The effect of nitriding time on hardness for group 2 (tempered, 670 °C, 50 l/h, air cooling)

The microstructure of this set of tools, as shown in Fig. 4 exhibits precipitation and concentration of carbides. The ferrite phase transforms into granulated cementite in tool no. i11 and to austenite in tool no. Sh-5, while tool no. Sh-4 converts to pearlite.



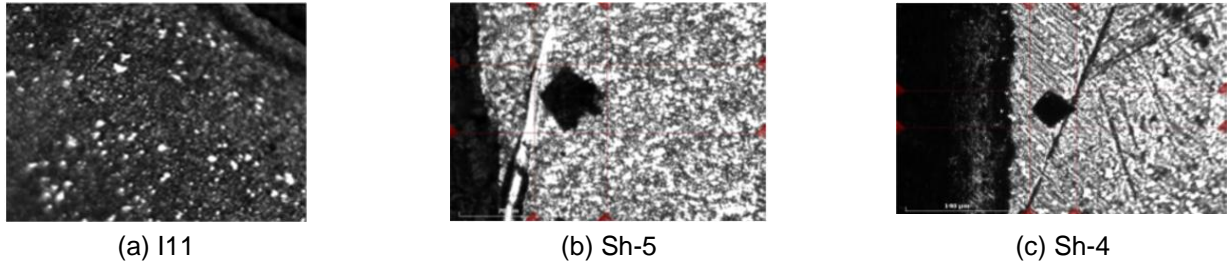


Fig. 4. The microstructure of group 2 (tempered, 670 °C, 50 l/h, air cooling)

**3.1.3 Group no. 3**

In Fig. 5 below the hardness at the nitriding time of 24 h, is the lowest (833.98 HV,) and at the time of 18 h is the highest (1332.84 HV). The relation between nitriding length of time and micro-hardness is almost inversely proportional, meaning that increasing the time is useless at these nitriding variables (tempered, 670 °C, 20 l/h, furnace cooling).

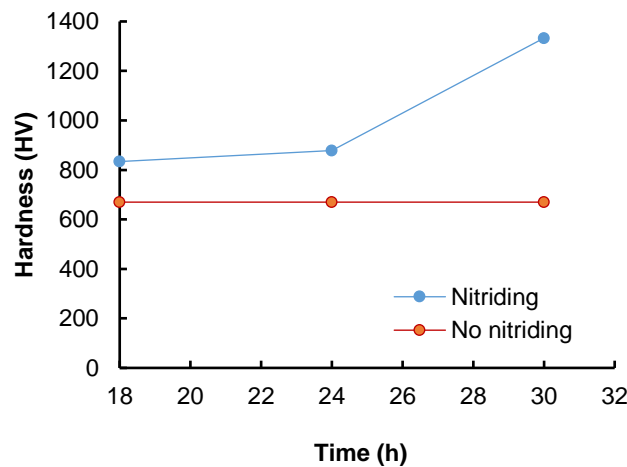


Fig. 5. The effect of nitriding time on hardness for group 3 (tempered,670 °C ,20 l/h, furnace cooling)

The microstructure of this group shown in Fig. 6. was modified to the cementite phase in tools no. L11 and Q11, but in tool no. Sh-3 the structure is coarse and the grains are bigger and converted to martensite.

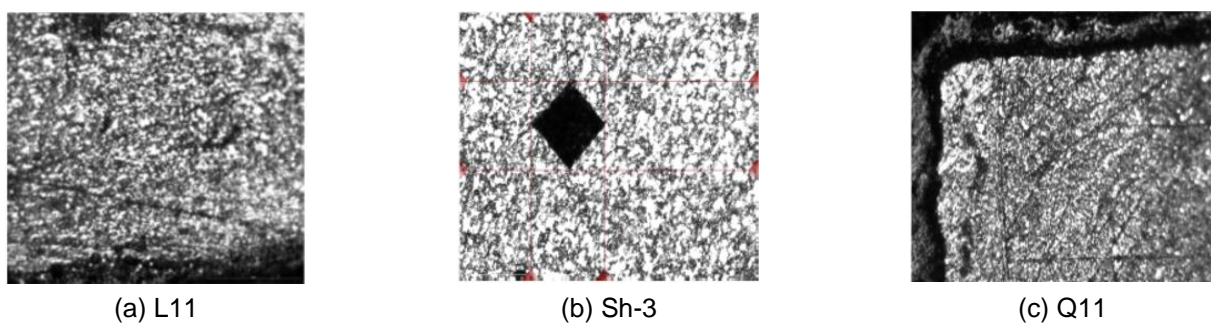


Fig. 6. The microstructure of group 3 (tempered, 670 °C, 20 l/h, furnace cooling)

**3.1.4 Group no. 4**

As shown in Fig. 7 the micro-hardness provides the superior value (1566.65 HV) with a flow of 110 l/h and the lower value (717.95 HV) at a flow of 50 l/h. It also illustrates the pattern and form of the increase in comparison to the untreated tool.

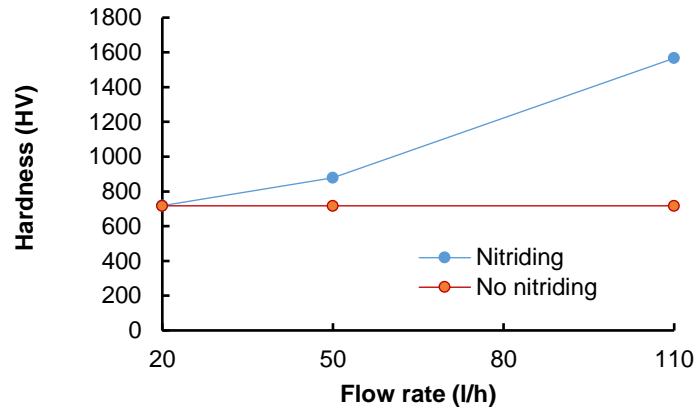


Fig. 7. The effect of nitrogen flow rate on micro-hardness for group 4 (tempered, 670 °C, 30 h)

The relationship between nitrogen flow and micro-hardness is almost directly proportional, which means that when the flow increases the microhardness increases, at these nitriding parameters (tempered, 670 °C, 30 h). The microstructure of this group shown in Fig. 8 was modified to the cementite phase.

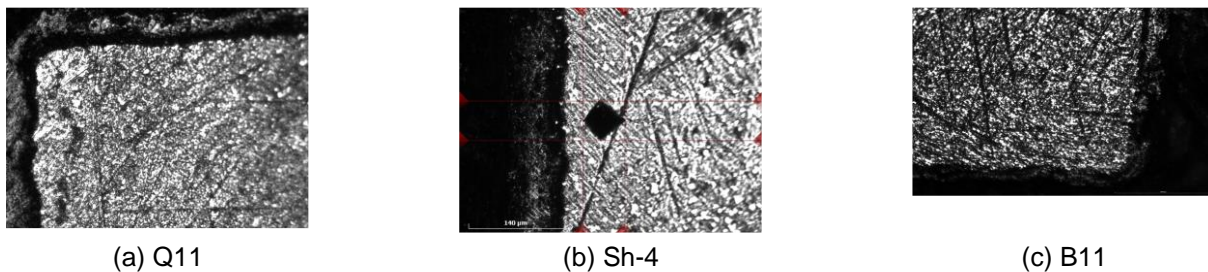


Fig. 8. The microstructure of group 4 (tempered, 670 °C, 30 h)

### 3.1.5 Group no 5.

The micro-hardness highest value was recorded at 20 l/h of nitrogen flow rate and the lowest was at 110 l/h as shown in fig. 9.

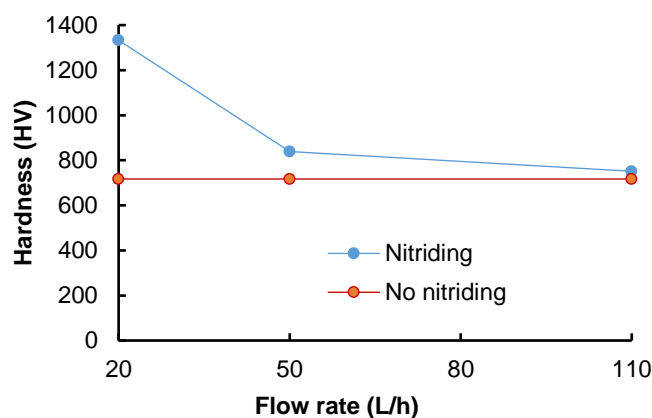


Fig. 9. The effect of flow rate on micro-hardness for group 5 (tempered, 670 °C, 18 h)

The micro-hardness in Fig. 9 shows that the relationship between the hardness and nitrogen flow at (tempered, 670 °C, 18 h) is fully inverse proportional. The higher the flow, the lower the hardness, and this can be explained by that, when the flow is low (20 l/h) at a short nitriding time of 18 h, all the nitrogen atoms move freely, and take place in the ferrite lattice more than the higher flow of nitrogen (110 l/h).

The white layer appears clearly in tool no. Sh-1, as shown in Fig.10 means that the reaction of nitrogen with iron and the formation of iron nitride mixture of iron nitrides  $\gamma'$ -Fe<sub>4</sub>N and/or  $\epsilon$ -Fe<sub>2,3</sub>N but the big increase of nitride layer doesn't always mean a good impression because the ferrite concentration decrease.

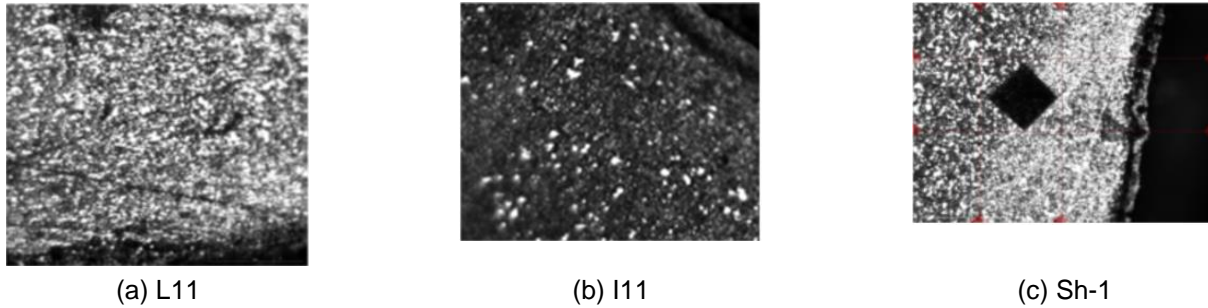


Fig. 10. The microstructure of group 5 (tempered, 670 °C, 18 h)

**3.1.6 Group no. 6**

The micro-hardness is the highest (902.28 HV) at the flow of 110 l/h and the lowest (785.27 HV) at the flow of 50 l/h as shown in Fig. 11 the nitriding process increases the micro-hardness, the relationship between flow and hardness in this group of cutting tools is almost direct. the higher the flow, the higher the hardness values.

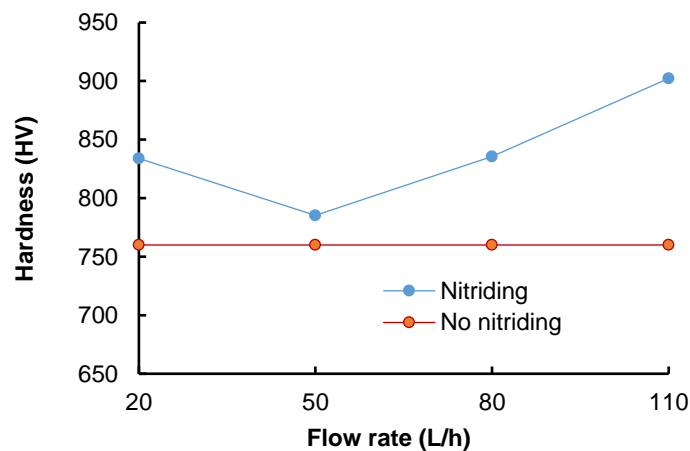


Fig. 11. The effect of flow rate on micro-hardness for group 6 (tempered, 670 °C, 24 h, in each flow)

In Fig. 12 the micro-structure of group 6 is shown, and the structure of tool no. Sh-3 is coarse and transformed to martensite, and austenite in tools no. Sh-5, tool no. H11 transformed to granular cementite, tool no. A11 transformed into a needle martensitic structure at the compound layer.

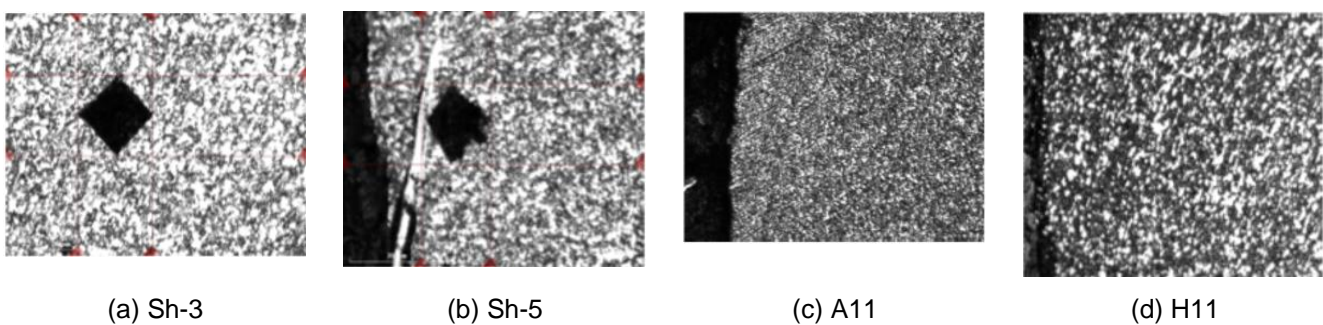


Fig. 12. The microstructure of group 6 (tempered, 670 °C, 24 h)

**3.1.7 Group no. 7**

As shown in Fig. 13 the lowest micro-hardness value for this group is 751.32 HV at 18 h, and the highest value is 1566.65 HV at 30 h. This indicates that when all the parameters are fixed at 670 °C for temperature, 110 l/h for flow rate, and tempering before nitriding, the results are consistent.



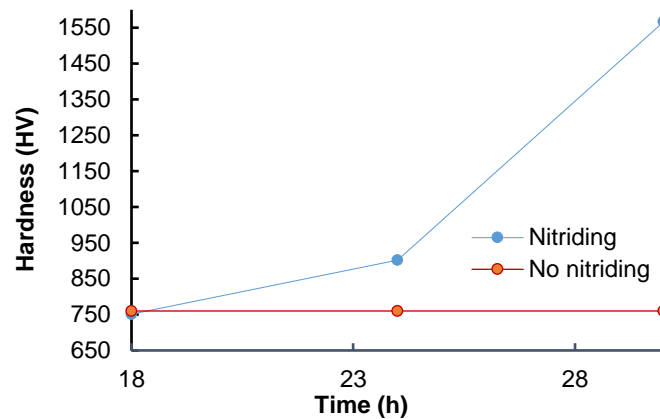


Fig.13. The effect of nitriding time on micro-hardness for group 7 (tempered, 670 °C,110 l/h)

The results demonstrate a direct relationship between the hardness values and the nitriding time; as a result, longer nitriding times correspond to higher hardness values. Conversely, the nitriding process increased the cutting tool's hardness when compared to its pre-nitriding state.

The microstructure of group 7 is shown in Fig. 14. The white layer is visible in tool no. Sh-1, and the microstructure of tools B11 and H11 also transition to a granular cementite phase. The reason for this is that when nitrogen reacts with iron, iron nitride mixtures of iron nitrides  $\gamma'$ - $Fe_4N$  and/or  $\epsilon$ - $Fe_{2,3}N$  are formed.

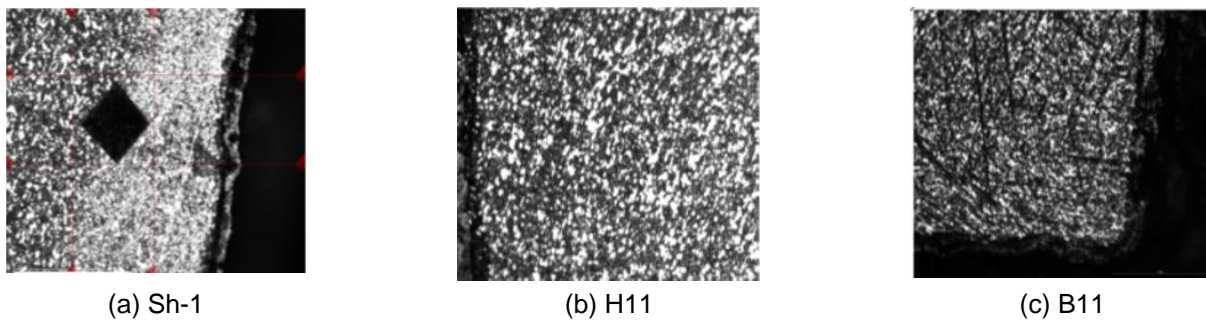


Fig. 14. The microstructure of group 7 (tempered, 670 °C, 110 l/h)

In tool Sh-1 the near-surface zone and the inner core zone have extremely different microstructures; the thick compound layer explains the decrease in microhardness.

### 3.1.8 Group no. 8

According to Fig.15, the micro-hardness of the tool increased to a high value of 1555.44 HV after it was quenched, and decreased to a low value of 795.93 HV after it was cooled in free air to room temperature.

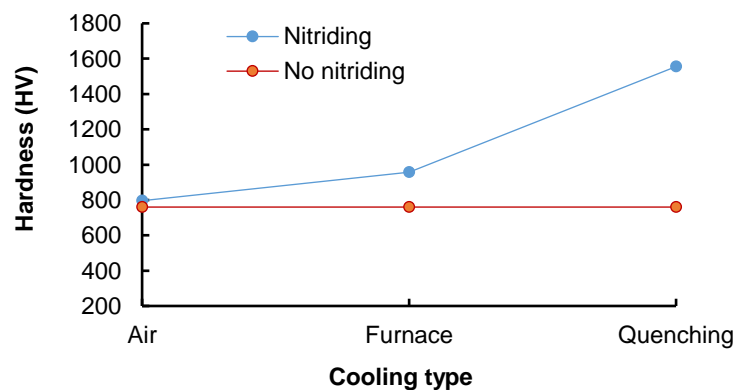


Fig. 15. The effect of cooling type on microhardness for group 8 (670 °C, 72h, 20 l/h, different cooling types)

The micro-hardness of the tool is increased by all types of cooling, and the micro-hardness values of air cooling and furnace cooling are similar.

Because quenching stops the process of recrystallization, the microstructure of a partially recrystallized tool is partially recrystallized. However, the micro-structure of the air-cooled tool has recrystallized because the process is taking enough time. Regarding the instrument that cools in the furnace, as seen in Fig. 16 the grains begin to grow.

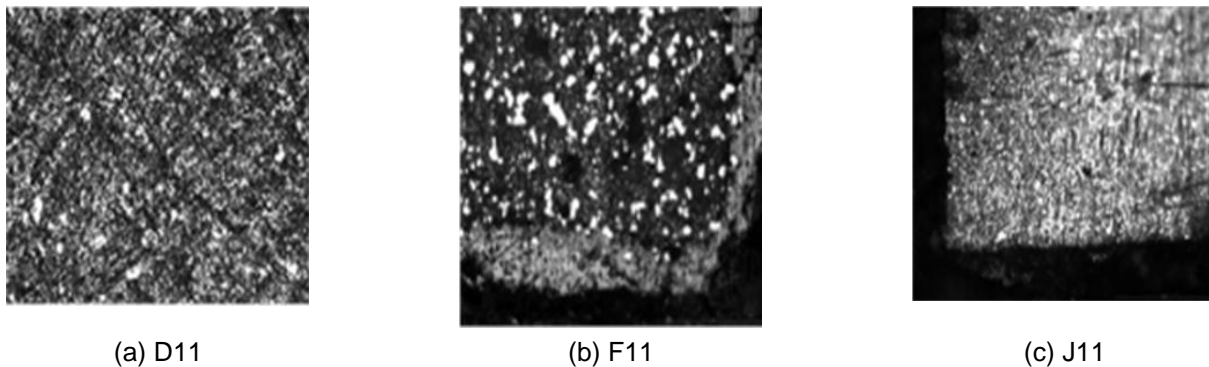


Fig. 16. The effect of cooling types on the microstructure of group 8 (670 °C, 72h, 20 l/h)

From the test results, we can see that the gas nitriding process increases the micro-hardness. The red line in the figures represents the untreated tools' hardness value, and at tool no. E11, the hardness value reaches its maximum value (2000HV). The micro-hardness value of the cutting tools from Sh-5 to E11 is higher than the untreated tools' micro-hardness.

In the case of the micro-hardness value of 2000 HV, tool no. E11 is placed into the furnace for 42 h at 670 °C and has a nitrogen flow rate of 20 l/h without prior treatment. After that, it is cooled in free air to obtain a very hard brittle layer. Similarly, in the case of a micro-hardness value of 717.98 HV, tool no. E11 is placed into the furnace for 30 h at 670 °C and a nitrogen flow rate of 50 l/h before being cooled in free air.

All of these nitriding processes are a good choice to improve the micro-hardness of cutting tools since the micro-hardness of tools from Sh-5 to E11 is higher than those of untreated tools. With a temperature of 670 °C and a flow rate of 20 l/h, tool no. K11 has an intermediate micro-hardness value (896.22 HV). To obtain these values, the tool was placed directly into the furnace for 30 h. For tool no. E11, the maximum value of micro-hardness is 2000 HV. Using the following equation (1), we can calculate the percentage increase in micro-hardness

$$\text{Hardness increase} = \frac{\text{HV after nitriding} - \text{HV before nitriding}}{\text{HV before nitriding}} \times 100 \% \quad (1)$$

$$\text{Hardness increase} = \frac{2000 - 759.76}{759.76} \times 100 \% = 1.63 \%$$

The hardness values from the outer edge to the base material vary in a certain pattern after nitriding, as proven by tool no. N11; in Fig. 17, the micro-hardness values are measured diagonally from one edge to another; and the test line's length is  $\sqrt{2}$  cm. As shown in Fig. 18, the five-point result indicates that hardness reduced until it reached the core and then increased till the opposite edge.



Fig .17. The direction and points of the micro-hardness test

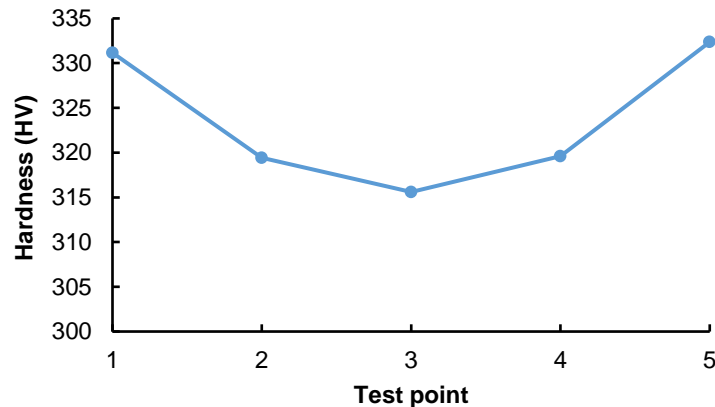


Fig. 18. Microhardness concerning the test point

### 3.2 Summary of the results

Table 4 provides an overview of the micro-hardness results for both the best and worst values, both before and after nitriding.

Table 4. Results summary

Before nitriding				
Microhardness 759.76 HV, tool A1				
After nitriding				
Micro hardness's best value is (2000 HV) at				
Specimen symbol	Time (h)	Cooling type	Nitrogen flow (l/h)	Heat treatment before nitriding
E11	42	Air	20	None
Micro hardness's worst value is (717.95 HV) at				
Specimen symbol	Time (h)	Cooling type	Nitrogen flow (l/h)	Heat treatment before nitriding
Sh-4	30	Air	50	Tempered

As indicated in Table. 5, the impact of nitriding on cutting tool wear was also evaluated by weighing the tools both before and after a turning operation for a pair of tools: one selected at random after nitriding and the other before. A weight percentage decrease calculation was done. The cutting parameters were: water cooling, 5 cm of cut length, 1 cm of cut depth, and 1000 rpm rotational speed.

Table 5. The effect of nitriding on tool wear

Before nitriding				
Microhardness 759.76 HV, wear /cutting time 0.00008 g/s, tool A1				
After nitriding				
The wear/cutting time value is 0.00004 g/s with a 50% decrease at				
Specimen symbol	Time (h)	Cooling type	Nitrogen flow (l/h)	Heat treatment before nitriding
Random specimen after nitriding (K11)	30	Air cooling	20	None

## 4 CONCLUSIONS

In general, the nitriding process improves the machinability. This result was assured in this study by the tests carried out after the nitriding process, which is the wear, and micro-hardness. The wear loss of cutting tools decreased and wear resistance improved by 50%.

Micro-hardness best result was 2000 HV, at a nitriding time of 42 h, the flow of nitrogen 20 l/h, and air cooling after nitriding with an increase of 1.63%.

The microstructure of the tools is improved by increasing the concentration of iron nitride in the ferrite cell.

All specimens exhibited higher hardness values than the untreated ones, according to the micro-hardness values for all nitrided tools. This implies that all nitriding procedures are suitable for enhancing the overall micro-hardness of cutting tools and that nitriding settings can be adjusted to produce acceptable outcomes.

Gas nitriding is the most effective method to improve the tool surface, especially for complex shapes that need identical hardening of the tool surface.

## 5 ACKNOWLEDGMENT

We gratefully acknowledge the support provided by Mutah University.

## 6 REFERENCES

- [1] Özel, T., & Karpat, Y. (2005). Predictive modeling of surface roughness and tool wear in hard turning using regression and neural networks. *International journal of machine tools and manufacture*, 45(4-5), 467-479. <https://doi.org/10.1016/j.ijmachtools.2004.09.007>
- [2] Ezugwu, E. O. (2005). Key improvements in the machining of difficult-to-cut aerospace superalloys. *International Journal of Machine Tools and Manufacture*, 45(12-13), 1353-1367. <https://doi.org/10.1016/j.ijmachtools.2005.02.003>
- [3] Akhtar, S. S., & Arif, A. (2010). Evaluation of gas nitriding process with in-process variation of nitriding potential for AISI H13 tool steel. *The International Journal of Advanced Manufacturing Technology*, 47, 687-698. DOI 10.1007/s00170-009-2215-4
- [4] Şirin, Ş. & Sarıkaya, M., (2021). Machinability performance of nickel alloy X-750 with SiAlON ceramic cutting tool under dry, MQL and hBN mixed nanofluid-MQL. *Tribology International*, 153, 106673. <https://doi.org/10.1016/j.triboint.2020.106673>
- [5] Da Silva Savonov, & G., Camarinha, (2019). Study of the influence of the RRA thermal treatment and plasma nitriding on corrosion behavior of 7075-T6 aluminum alloy. *Surface and Coatings Technology*, 374, 736-744. <https://doi.org/10.1016/j.surfcoat.2019.04.095>
- [6] Fu, Y., & Liao, Y. (2022). Layer structured materials for ambient nitrogen fixation. *Coordination Chemistry Reviews*, 460, 214468. <https://doi.org/10.1016/j.ccr.2022.214468>
- [7] Wang, L., & Chen, W. (2019). Surface strategies for catalytic CO<sub>2</sub> reduction: from two-dimensional materials to nanoclusters to single atoms. *Chemical Society Reviews*, 48(21), 5310-5349 <https://doi.org/10.1039/C9CS00163H>
- [8] Tu, L., & Tian, S. (2020). Cutting performance of cubic boron nitride-coated tools in dry turning of hardened ductile iron. *Journal of manufacturing processes*, 56, 158-168. <https://doi.org/10.1016/j.jmapro.2020.04.081>
- [9] Özel, T., & Biermann, D. (2021). Structured and textured cutting tool surfaces for machining applications. *CIRP Annals*, 70(2), 495-518. <https://doi.org/10.1016/j.cirp.2021.05.006>
- [10] Fouathiya A, Meziani S, Sahli M, Barrière T. (2021) Experimental investigation of microtextured cutting tool performance in titanium alloy via turning. *Journal of Manufacturing Processes*;69:33-46. <https://doi.org/10.1016/j.jmapro.2021.07.030>
- [11] Gordon, S. & Lahiff, C. (2019). The Effect of High-Speed Machining on the Crater Wear Behaviour of PCBN Tools in Hard Turning. *Procedia Manufacturing*, 38, 1833-1848. <https://doi.org/10.1016/j.promfg.2020.01.076>
- [12] Dolinšek S, Šuštaršič B, Kopač J. (2001) Wear mechanisms of cutting tools in high-speed cutting processes. *Wear*;250(1-12):349-56. [https://doi.org/10.1016/S0043-1648\(01\)00620-2](https://doi.org/10.1016/S0043-1648(01)00620-2)
- [13] Cheng, Y., & Ding, Y. (2022). Simulation and experimental study of tool wear and damage in milling SA 508III steel. *Surface Topography: Metrology and Properties*, 10(3), 035033. DOI 10.1088/2051-672X/ac9073
- [14] Sarıkaya, M., & Gupta, M. K. (2021). A state-of-the-art review on tool wear and surface integrity characteristics in machining of superalloys. *CIRP Journal of Manufacturing Science and Technology*, 35, 624-658. <https://doi.org/10.1016/j.cirpj.2021.08.005>
- [15] Szczotkarz, N., & Mrugalski, R. (2021). Cutting tool wear in turning 316L stainless steel in the conditions of minimized lubrication. *Tribology International*, 156, 106813. <https://doi.org/10.1016/j.triboint.2020.106813>
- [16] de Araújo, E., Bandeira, R. M., Manfrinato, M. D., Moreto, J. A., Borges, R., dos Santos Vales, S., Suzuki, P. A., & Rossino, L. S. (2019). Effect of ionic plasma nitriding process on the corrosion and micro-abrasive wear behavior of AISI 316L austenitic and AISI 470 super-ferritic stainless steels. *Journal of Materials Research and Technology*, 8(2), 2180-2191. <https://doi.org/10.1016/j.jmrt.2019.02.006>
- [17] Fu, Y., & Liao, Y. (2022). Layer structured materials for ambient nitrogen fixation. *Coordination Chemistry Reviews*, 460, 214468. <https://doi.org/10.1016/j.ccr.2022.214468>
- [18] Venkatesan, K., Devendiran, S. (2020). Investigation of machinability characteristics and comparative analysis under different machining conditions for sustainable manufacturing. *Measurement*, 154, 107425. <https://doi.org/10.1016/j.measurement.2019.107425>



- [19] Bloyce, A. (1998). Surface engineering of titanium alloys for wear protection. *Proceedings of the Institution of Mechanical Engineers, Part J: Journal of Engineering Tribology*, 212(6), 467-476. <https://doi.org/10.1243/1350650981542263>
- [20] Şap, E., Usca, U. A. (2021). Tool wear and machinability investigations in dry turning of Cu/Mo-SiCp hybrid composites. *The International Journal of Advanced Manufacturing Technology*, 114(1), 379-396. <https://doi.org/10.1007/s00170-021-06889-8>
- [21] Xu, Z., Huang, J., Xu. (2020). Plasma surface metallurgy of materials based on double glow discharge phenomenon. *arXiv preprint arXiv:2003.10250*. <https://doi.org/10.48550/arXiv.2003.10250>
- [22] Chiang, W. H., Mariotti, D. (2020). Microplasmas for advanced materials and devices. *Advanced Materials*, 32(18), 1905508. <https://doi.org/10.1002/adma.201905508>
- [23] Eng, A. Y. S., Kumar, V., Zhang, Y., Luo, J., Wang, W., Sun, Y., Li, W., & Seh, Z. W. (2021). Room-temperature sodium-sulfur batteries and beyond: Realizing practical high energy systems through anode, cathode, and electrolyte engineering. *Advanced Energy Materials*, 11(14), 2003493. <https://doi.org/10.1002/aenm.202003493>
- [24] Cojocar, M. O., Branzei, M. (2021). Sulfonitrocarburizing of High-Speed Steel Cutting Tools: *Kinetics and Performances*. *Materials*, 14(24), 7779. <https://doi.org/10.3390/ma14247779>
- [25] Fouathia, A., Meziani, S. (2021). Experimental investigation of microtextured cutting tool performance in titanium alloy via turning. *Journal of Manufacturing Processes*, 69, 33-46. <https://doi.org/10.1016/j.jmapro.2021.07.030>
- [26] Günay, M., Korkmaz, M. (2020). Performance analysis of coated carbide tool in turning of Nimonic 80A superalloy under different cutting environments. *Journal of Manufacturing Processes*, 56, 678-687. <https://doi.org/10.1016/j.jmapro.2020.05.031>
- [27] Astakhov, V. P. (2004). The assessment of cutting tool wear. *International journal of machine tools and manufacture*, 44(6), 637-647. <https://doi.org/10.3390/pr8091056>
- [28] Evseev, N., Ziatdinov, M. (2020). Process of obtaining chromium nitride in the combustion mode under conditions of co-flow filtration. *Processes*, 8(9), 1056. <https://doi.org/10.3390/pr8091056>
- [29] Rath, D., & Panda, S. (2022). Analysis and prediction of tool wear in dry turning of hardened D3 steel using hybrid insert: A novel wear map approach. *Proceedings of the Institution of Mechanical Engineers, Part B: Journal of Engineering Manufacture*, 236(10), 1355-1367. <https://doi.org/10.1177/09544054221076242>
- [30] Poulachon, G., Moisan, A. (2001). Tool-wear mechanisms in hard turning with polycrystalline cubic boron nitride tools. *Wear*, 250(1-12), 576-586. [https://doi.org/10.1016/S0043-1648\(01\)00609-3](https://doi.org/10.1016/S0043-1648(01)00609-3)

Paper submitted: 10.04.2024.

Paper accepted: 19.07.2024.

This is an open access article distributed under the CC BY 4.0 terms and conditions